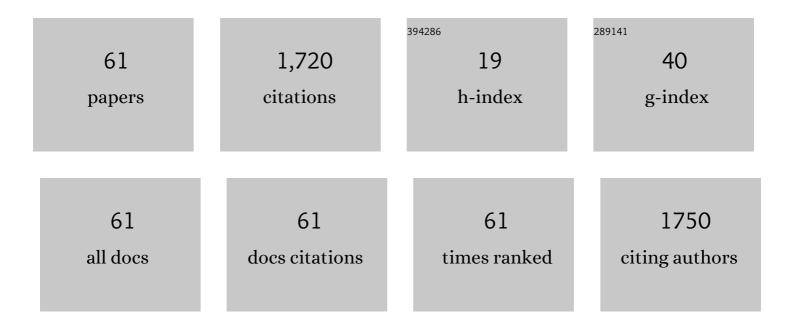
## Sebastian Weingärtner

List of Publications by Year in descending order

Source: https://exaly.com/author-pdf/2748982/publications.pdf Version: 2024-02-01



#	Article	IF	CITATIONS
1	Accuracy, Precision, and Reproducibility of Four T1 Mapping Sequences: A Head-to-Head Comparison of MOLLI, ShMOLLI, SASHA, and SAPPHIRE. Radiology, 2014, 272, 683-689.	3.6	255
2	Scanâ€specific robust artificialâ€neuralâ€networks for kâ€space interpolation (RAKI) reconstruction: Databaseâ€free deep learning for fast imaging. Magnetic Resonance in Medicine, 2019, 81, 439-453.	1.9	253
3	Combined saturation/inversion recovery sequences for improved evaluation of scar and diffuse fibrosis in patients with arrhythmia or heart rate variability. Magnetic Resonance in Medicine, 2014, 71, 1024-1034.	1.9	149
4	T1 mapping in cardiac MRI. Heart Failure Reviews, 2017, 22, 415-430.	1.7	97
5	Freeâ€breathing multislice native myocardial T <sub>1</sub> mapping using the sliceâ€interleaved T <sub>1</sub> (STONE) sequence. Magnetic Resonance in Medicine, 2015, 74, 115-124.	1.9	83
6	Myocardial T1-mapping at 3T using saturation-recovery: reference values, precision and comparison with MOLLI. Journal of Cardiovascular Magnetic Resonance, 2016, 18, 84.	1.6	70
7	Adaptive registration of varying contrastâ€weighted images for improved tissue characterization (ARCTIC): Application to T <sub>1</sub> mapping. Magnetic Resonance in Medicine, 2015, 73, 1469-1482.	1.9	63
8	Improved quantitative myocardial T <sub>2</sub> mapping: Impact of the fitting model. Magnetic Resonance in Medicine, 2015, 74, 93-105.	1.9	57
9	Joint myocardial T <sub>1</sub> and T <sub>2</sub> mapping using a combination of saturation recovery and T <sub>2</sub> â€preparation. Magnetic Resonance in Medicine, 2016, 76, 888-896.	1.9	57
10	Magnetic resonance fingerprinting using echoâ€planar imaging: Joint quantification of T <sub>1</sub> and relaxation times. Magnetic Resonance in Medicine, 2017, 78, 1724-1733.	1.9	55
11	Diffusion parameter mapping with the combined intravoxel incoherent motion and kurtosis model using artificial neural networks at 3ÂT. NMR in Biomedicine, 2017, 30, e3833.	1.6	49
12	Freeâ€breathing postâ€contrast threeâ€dimensional T <sub>1</sub> mapping: Volumetric assessment of myocardial T <sub>1</sub> values. Magnetic Resonance in Medicine, 2015, 73, 214-222.	1.9	35
13	Simultaneous multislice imaging for native myocardial T <sub>1</sub> mapping: Improved spatial coverage in a single breath-hold. Magnetic Resonance in Medicine, 2017, 78, 462-471.	1.9	32
14	On the selection of sampling points for myocardial T <sub>1</sub> mapping. Magnetic Resonance in Medicine, 2015, 73, 1741-1753.	1.9	31
15	Time efficient whole-brain coverage with MR Fingerprinting using slice-interleaved echo-planar-imaging. Scientific Reports, 2018, 8, 6667.	1.6	29
16	Freeâ€breathing combined threeâ€dimensional phase sensitive late gadolinium enhancement and T <sub>1</sub> mapping for myocardial tissue characterization. Magnetic Resonance in Medicine, 2015, 74, 1032-1041.	1.9	27
17	Low-Rank Tensor Models for Improved Multidimensional MRI: Application to Dynamic Cardiac \$T_1\$ Mapping. IEEE Transactions on Computational Imaging, 2020, 6, 194-207.	2.6	27
18	Accelerated coronary MRI with sRAKI: A database-free self-consistent neural network k-space reconstruction for arbitrary undersampling. PLoS ONE, 2020, 15, e0229418.	1.1	25

#	Article	IF	CITATIONS
19	Temporally resolved parametric assessment of Zâ€magnetization recovery (TOPAZ): Dynamic myocardial T <sub>1</sub> mapping using a cine steadyâ€state lookâ€locker approach. Magnetic Resonance in Medicine, 2018, 79, 2087-2100.	1.9	24
20	Impact of motion correction on reproducibility and spatial variability of quantitative myocardial T2 mapping. Journal of Cardiovascular Magnetic Resonance, 2015, 17, 46.	1.6	21
21	Development, validation, qualification, and dissemination of quantitative MR methods: Overview and recommendations by the ISMRM quantitative MR study group. Magnetic Resonance in Medicine, 2022, 87, 1184-1206.	1.9	21
22	Magnetic resonance fingerprinting for simultaneous renal <i>T</i> <sub>1</sub> and <i>T</i> <sub>2</sub> <sup>*</sup> mapping in a single breathâ€hold. Magnetic Resonance in Medicine, 2020, 83, 1940-1948.	1.9	18
23	Cardiac MR: From Theory to Practice. Frontiers in Cardiovascular Medicine, 2022, 9, 826283.	1.1	18
24	Oxygen extraction fraction mapping at 3 Tesla using an artificial neural network: A feasibility study. Magnetic Resonance in Medicine, 2018, 79, 890-899.	1.9	15
25	Emerging Techniques in Cardiac Magnetic Resonance Imaging. Journal of Magnetic Resonance Imaging, 2022, 55, 1043-1059.	1.9	14
26	Gaussian signal relaxation around spin echoes: Implications for precise reversible transverse relaxation quantification of pulmonary tissue at 1.5 and 3 Tesla. Magnetic Resonance in Medicine, 2017, 77, 1938-1945.	1.9	13
27	Accelerated Coronary Mri Using 3D Spirit-Raki With Sparsity Regularization. , 2019, 2019, 1692-1695.		13
28	Black-blood native T <sub>1</sub> mapping: Blood signal suppression for reduced partial voluming in the myocardium. Magnetic Resonance in Medicine, 2017, 78, 484-493.	1.9	12
29	Saturation-Recovery Myocardial T1-Mapping during Systole: Accurate and Robust Quantification in the Presence of Arrhythmia. Scientific Reports, 2018, 8, 5251.	1.6	12
30	Accelerated white matter lesion analysis based on simultaneous <i>T</i> <sub>1</sub> and <i>T</i> <sub>2</sub> <sup>â^—</sup> quantification using magnetic resonance fingerprinting and deep learning. Magnetic Resonance in Medicine, 2021, 86, 471-486.	1.9	12
31	Scan time reduction in 23Na-Magnetic Resonance Imaging using the chemical shift imaging sequence: Evaluation of an iterative reconstruction method. Zeitschrift Fur Medizinische Physik, 2015, 25, 275-286.	0.6	11
32	Motion-robust cardiac B1+ mapping at 3T using interleaved bloch-siegert shifts. Magnetic Resonance in Medicine, 2017, 78, 670-677.	1.9	11
33	Multi-scale locally low-rank noise reduction for high-resolution dynamic quantitative cardiac MRI. , 2017, 2017, 1473-1476.		11
34	Locally Low-Rank tensor regularization for high-resolution quantitative dynamic MRI. , 2017, 2017, .		11
35	Freeâ€breathing simultaneous <i>T</i> <sub>1</sub> , <i>T</i> <sub>2</sub> , and <i>T</i> <sub>2</sub> <sup>â^—</sup> quantification in the myocardium. Magnetic Resonance in Medicine, 2021, 86, 1226-1240.	1.9	11
36	Heart-rate independent myocardial T1-mapping using combined saturation and inversion preparation pulses. Journal of Cardiovascular Magnetic Resonance, 2013, 15, P46.	1.6	10

#	Article	IF	CITATIONS
37	Comparison of spoiled gradient echo and steadyâ€state freeâ€precession imaging for native myocardial <i>T</i> <sub>1</sub> mapping using the sliceâ€interleaved <i>T</i> <sub>1</sub> mapping (STONE) sequence. NMR in Biomedicine, 2016, 29, 1486-1496.	1.6	10
38	Improved simultaneous multislice cardiac MRI using readout concatenated kâ€space SPIRiT (ROCKâ€SPIRiT). Magnetic Resonance in Medicine, 2021, 85, 3036-3048.	1.9	10
39	Accelerated Simultaneous Multi-Slice MRI using Subject-Specific Convolutional Neural Networks. , 2018, 2018, 1636-1640.		6
40	Scan-Specific Residual Convolutional Neural Networks for Fast MRI Using Residual RAKI. , 2019, , .		6
41	Improved Regularized Reconstruction for Simultaneous Multi-Slice Cardiac MRI T <sub>1</sub> Mapping. , 2019, 2019, .		6
42	Optimized fast GPU implementation of robust artificial-neural-networks for k-space interpolation (RAKI) reconstruction. PLoS ONE, 2019, 14, e0223315.	1.1	6
43	Improved Simultaneous Multi-Slice Imaging for Perfusion Cardiac MRI Using Outer Volume Suppression and Regularized Reconstruction. , 2020, , .		4
44	Accuracy and reproducibility of four T1 mapping sequences: a head-to-head comparison of MOLLI, ShMOLLI, SASHA, and SAPPHIRE. Journal of Cardiovascular Magnetic Resonance, 2014, 16, O26.	1.6	3
45	Black-blood T1 mapping at 3T: Reduced partial-voluming using adiabatic MSDE preparation. Journal of Cardiovascular Magnetic Resonance, 2016, 18, W5.	1.6	3
46	Fast GPU Implementation of a Scan-Specific Deep Learning Reconstruction for Accelerated Magnetic Resonance Imaging. , 2018, 2018, 399-403.		3
47	Towards measuring the effect of flow in blood <i>T</i> <sub>1</sub> assessed in a flow phantom and <i>i&gt;in vivo</i> . Physics in Medicine and Biology, 2020, 65, 095001.	1.6	3
48	Motion correction for free breathing quantitative myocardial t2 mapping: impact on reproducibility and spatial variability. Journal of Cardiovascular Magnetic Resonance, 2015, 17, W5.	1.6	2
49	Functional MRI of neuro-electro-magnetic oscillations: Statistical processing in the presence of system imperfections. , 2021, , .		2
50	Improved 3D late gadolinium enhancement MRI for patients with arrhythmia or heart rate variability. Journal of Cardiovascular Magnetic Resonance, 2013, 15, P29.	1.6	1
51	Selection of sampling points for saturation recovery based myocardial T1 mapping. Journal of Cardiovascular Magnetic Resonance, 2014, 16, W32.	1.6	1
52	Subject-Specific Convolutional Neural Networks for Accelerated Magnetic Resonance Imaging. , 2018, 2018, .		1
53	Magnetic Resonance Imaging compatible Elastic Loading Mechanism (MELM): A minimal footprint device for MR imaging under load. , 2021, 2021, 3721-3724.		1
54	Detection of left ventricular diffuse fibrosis with quantitative T1 mapping in patients with paroxysmal atrial fibrillation. Journal of Cardiovascular Magnetic Resonance, 2013, 15, P117.	1.6	0

#	Article	IF	CITATIONS
55	Joint image reconstruction and motion parameter estimation for free-breathing navigator-gated cardiac MRI. Proceedings of SPIE, 2013, , .	0.8	0
56	Joint myocardial T1 and T2 mapping. Journal of Cardiovascular Magnetic Resonance, 2015, 17, Q1.	1.6	0
57	Reproducibility of free-breathing multi-slice native myocardial T1 mapping using the slice-interleaved T1 (STONE) sequence. Journal of Cardiovascular Magnetic Resonance, 2015, 17, W29.	1.6	0
58	Free-breathing myocardial T1 mapping using magnetization-prepared slice interleaved spoiled gradient echo imaging. Journal of Cardiovascular Magnetic Resonance, 2015, 17, W7.	1.6	0
59	Robust Online Spike Recovery for High-Density Electrode Recordings using Convolutional Compressed Sensing. , 2019, , .		0
60	Functional LGE Imaging: Cardiac Phase-Resolved Assessment of Focal Fibrosis. , 2019, 2019, 3999-4003.		0
61	Saturation-pulse prepared heart-rate independent inversion-recovery (SAPPHIRE) biventricular T1 mapping: inter-field strength, head-to-head comparison of diastolic, systolic and dark-blood measurements. BMC Medical Imaging, 2022, 22, .	1.4	0